Natuna Off-Shelf Current (NOC) Vertical Variability and Its Relation to ENSO in the North Natuna Sea

Hariyadi[1,2*], Johanes Hutabarat[3], Denny Nugroho Sugianto[1,4], Muhammad Faiq Marwa Noercholis[1], Niken Dwi Prasetyani,[1] Widodo S. Pranowo[5], Kunarso[1], Parichat Wetchayount[6], Anindya Wirasatriya[1,4]

[1]Department of Oceanography, Faculty of Fisheries and Marine Science, Diponegoro University
[2]Doctoral Program of Marine Science, Diponegoro University
[3]Department of Aquaculture, Faculty of Fisheries and Marine Science, Diponegoro University
[4]Center for Coastal Rehabilitation and Disaster Mitigation Studies (CoREM), Diponegoro University
Jl. Prof. H. Soedharto, SH, Tembalang Semarang. 50275 Indonesia
[5]Marine Research Center, Agency for Marine & Fisheries Research & Human Resources,
Ministry of Marine and Fisheries
Gedung Mina Bahari I 5th Floor, Jl. Medan Merdeka Timur No. 16 Jakarta Pusat 10110 Indonesia
[6]Department of Geography, Faculty of Social Science, Srinakharinwirot University
8 114 Sukhumvit 23, Bangkok, Thailand
Email: hariyadi@lecturer.undip.ac.id

Abstract

During the northwest monsoon (NWM), southerly flow off the Natuna Islands appeared as the extension of the turning Vietnam coastal jet, known as Natuna off-shelf current (NOC). NOC is generated by the interaction of wind stress and the North Natuna Sea's bottom topography. The purposes of the present study is to investigate the vertical variability of NOC and its relation to El Niño Southern Oscillation (ENSO) using Marine Copernicus reanalysis data. The vertical variability refers to the spatial distribution of NOC pattern at the surface layer, thermocline layer, and deep/bottom layer. in 2014 as representative of normal ENSO condition. To investigate the effect of ENSO, the spatial distribution of NOC in 2011 and 2016 were compared which represent the La Niña and El Niño conditions, respectively. The results show that NOC starts to generate at the southeast monsoon season to the transition I season and peaks in the northwest monsoon season. The occurrence of NOC is identified at all depth layers with the weakened NOC at the deep layer. Related to the ENSO effect, La Niña tends to strengthen NOC while El Niño tends to weaken NOC. These are releted with the strengthening and weakening northerly wind speed during La Niña and El Niño, Respectively. During La Niña events, the NOC occurs more frequently than during El Niño. Thus, beside affecting the magnitude of NOC, ENSO also influence the frequency occurrence of NOC.

Keywords: *Natuna off-shelf current (NOC), vertical variability, ENSO, North Natuna Sea*

Introduction

Lying on oceanic tectonic plates' confluence (the Eurasian Plate, the Indo-Australian Plate, and the Pacific Plate), Indonesian Archipelago experiences substantial seasonal variation driven by the monsoon system which the primary wind direction rotates every season (Susanto *et al*., 2006). Every dry season known as southeast monsoon (SEM) (June-August), the southeasterly wind blew from Australia to Eurasian Continent, carrying warm and dry air over Indonesian region. In contrast, during rainy season or northwest monsoon (NWM), the northwesterly wind from Eurasian continent carried warm and moist air over the Indonesian region during December-February (Setiawan and Habibie, 2010; Alifdini *et al*., 2021). The period from March to May and September to November is known as the first and the second transitional seasons. Thus, this monsoon system influences the dynamics of the Indonesian Seas in general.

North Natuna Sea is a marginal sea located in the northwestern part of the Indonesian Archipelago. Characterized by relatively shallow bathymetry (< 200 m), the North Natuna Sea is bordered by Malaysia Peninsula in the west, Kalimantan Island in the east, the Java Sea in the south, and the South China Sea in the north (Figure 1). Due to the direct entity with the South China Sea, the North Natuna Sea characteristics are very complex. In terms of ocean-atmosphere large-scale interactions, these areas are influenced by monsoon (Hu *et al*., 2000; Xue *et al*., 2004), El Nino Southern Oscillation (ENSO) (Wang *et al*., 2006a; Zu *et al*., 2019; Maisyarah *et al*., 2019), and Indian Ocean Dipole (IOD) (Khaldun *et al*., 2018).

*) Corresponding author

https://ejournal.undip.ac.id/index.php/ijms
DOI: 10.14710/ik.ijms.26.2.63-70
Received : 20-03-2021
Accepted : 11-05-2021

Li *et al*. (2003) defined the main annual variation of the circulation in North Natuna Sea as characterized by the occurrence of a cyclonic gyre in the northern South China Sea from November to April; Nansha Cyclone from November to February; Kuroshio intrusion from November to February; anticyclonic northward monsoon jet from May to July; cyclonic northward monsoon jet from August to October; Vietnam offshore current from August to October; and Natuna off-shelf current (NOC) from November to February.

Wyrtki (1961) firstly revealed NOC, describing the extension of Vietnam Coastal Jet (VCJ) resulting in the NOC circulation in the North Natuna Sea generating a cyclonic Eddy. Therefore, another study (Chu *et al*., 1999) defined this phenomenon as a Natuna Island Eddy (NIE). The NIE was more stable during the NWM with a maximum swirl velocity of 0.6 $m.s^{-1}$ and an average core velocity of 0.45–0.5 $m.s^{-1}$. In contrast, During the SEM, NIE turned to be weak anticyclonic Eddy. NOC plays important role for marine productivity since NOC brings nutrient rich waters to the euphotic zone (Yin *et al*., 2018).

The NOC pattern was mapped by Fang *et al*. (2002) who summarizing the previous studies related to the circulation in the South China Sea. More over, the observational evidence of NOC was initially announced by Fang *et al*. (2002), who conducting a survey using CTD and ADCP instruments associated with the winter cruise project (1989-1993). These studies determined the maximum geostrophic velocity of NOC (approximately 80 $cm.s^{-1}$) and the northeasterly winter wind stress. The northeasterly winter wind stress might contribute to the formation of upwind current (NOC) which generates the maximum pressure around the Natuna Islands. Furthermore, Fang *et al*. (2002) explained that the southern strait connecting to the Java Sea is shallow and narrow, forming the local converging topography which accumulates seawater over the southern shelf by the continuous forcing of strong winter northeasterly winds and in turn drives the water northward as NOC across the shelf edge near 112° E under the restriction of the east and west lateral boundaries. Thus, the generation of NOC was the result of interaction between wind stress and bottom topography.

Later on, the investigation of circulation pattern by using observational data and numerical models only focus at the South China Sea and mostly on the surface layer.(Guohong *et al*., 2005; Gan *et al*., 2006; Wang *et al*., 2006b; Fang *et al*., 2009; Tangang *et al*., 2011; Wei *et al*., 2016; and Zhu *et al*., 2019) which made the investigation of NOC was missed in their study. Thus, the vertical variability of NOC has not been well-documented yet. Therefore, this study aims to investigate the vertical variability of NOC and its relation to El Niño Southern Oscillation (ENSO) using reanalysis data. The vertical variability refers to the spatial distribution of NOC pattern at the surface layer, thermocline layer, and deep/bottom layer.

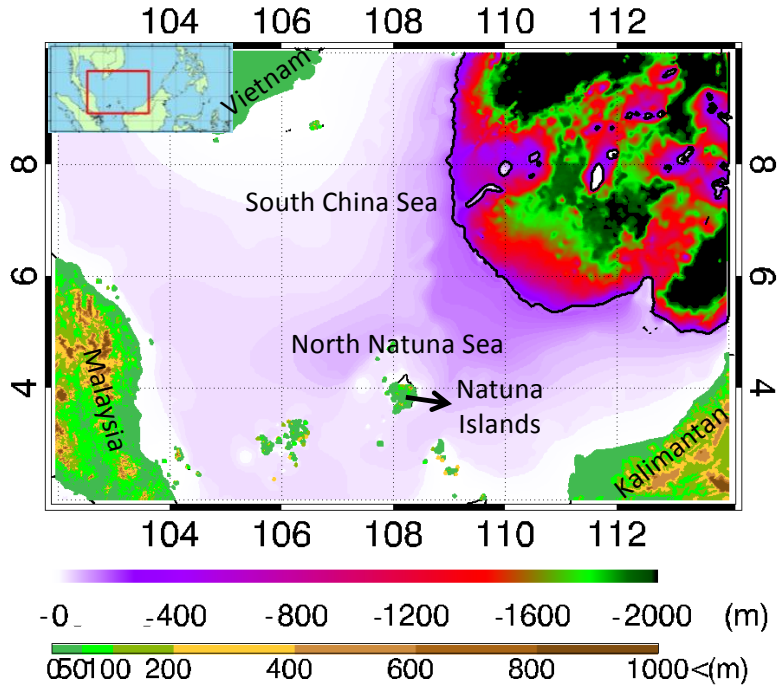

Figure 1. Bathymetry and topography of the study area. The black contour denotes isobath of 200 m.

Materials and Methods

Data

A set of Global Ocean Physics Reanalysis data (GLOBAL_REANALYSIS_PHY_ 001_030) from Marine Copernicus was employed in this study (Fernandez and Lellouche, 2018). Monthly ocean current and temperature data during 2006 – 2016 were used in this study. The grid interval of this dataset was 0.083° × 0.083° with 50 depth levels.These data were validated using *in situ* data and showed good accuracy. The Root mean square difference (RMSD) of sea current is generally lower than 0.25 $m.s^{-1}$ with the smaller RMSD at the upper layer equatorial vertical structure. Temperature profiles along the equator are very consistent with observations with RMSD generally smaller than 0.4° (Drevillon *et al*., 2018). For surface wind, a semi-daily Advanced Scatterometer (ASCAT) (Figa-Saldana *et al*., 2002) was used with the spatial resolution of 0.125° × 0.125°. Current, temperature, and surface wind data can be downloaded at https://resources.marine. copernicus. eu/?option=com_csw&task=results

Southern Oscillation Index (SOI) retrieved from a webpage: https://www.cpc.ncep.noaa.gov/data/ indi ces/soi were employed to correlate the effect of ENSO. SOI is a standardized index based on the observed sea level pressure differences between Tahiti and Darwin, Australia. The negative phase of the SOI represents below-normal (above-normal) air pressure at Tahiti (Darwin) (Ropelewski and Jones, 1987). Thus, the negative SOI values correspond with abnormally warm ocean waters across the eastern tropical Pacific typical of El Niño events. In contrast, the positive SOI values correspond to La Niña events.

Methods

The vertical section of temperature was plotted using Ocean Data View to determine the North Natuna Sea's vertical layers, as shown in Figure 2. The mixed layer was situated from the surface up to 40 m depth denoted by the isotherm layer of about 29°C. Below this layer, the temperature dropped significantly, characterized by the dense temperature contour from 40 m up to 100 m depth. This layer indicated the thermocline layer. At a depth of below 100 m, the bottom/deep layer was denoted by the stable temperature of <20^{o}C. Therefore, this study shows the spatial distribution of the current pattern at 0.49 m, 55.76 m, and 109.73 m depth to represent the surface layer, thermocline, and bottom/deep layer. The current pattern at each layer is descriptively analyzed by plotting using Interactive Data Language (IDL).

The analysis begins by showing the seasonal pattern of current at the different depth layers during the normal period of ENSO. Then, to examine the influence of ENSO, the NOC pattern was compared during strong El Niño and strong La Niña periods (Figure 3). The year of 2014, 2016, and 2011 were chosen as the observed period for normal condition, strong El Niño and strong La Niña, respectively. The surface wind pattern in 2011 and 2016 was displayed using IDL to obtain the mechanisms on how ENSO influence the variability of NOC.

Results and Discussion

Seasonal variation of NOC

To obtain the seasonal variation of NOC at the different depth layer, the current vector distribution during the normal ENSO period was plotted, as shown in Figure 4. During the NWM, the NOC showed the peak magnitude whereby the cyclonic eddy was also observed at 108°E - 112°E and 4°N - 8°N at the surface and thermocline layer. Strong VCJ extended to 6°N, between 108°E and 110°E with the maximum speed about 1 $m.s^{-1}$ at the surface layer. VCJ followed the isobath of 200 m in Figure 1 known as the western boundary current, Since in the northern part of Natuna Islands is shallow, the water piled up and finally the turning point at 110°E and 4°N was observed which then transformed to NOC throughout 110°E-112°E. This finding is in accordance with Fang *et al*. (2002) who emphasized that bottom topography is important for the generation of NOC. The maximum speed of NOC at the surface, thermocline and deep layer were about 0.6 $m.s^{-1}$, 0.5 $m.s^{-1}$, and 0.2 $m.s^{-1}$, respectively.

This finding indicates that the thermocline layer can reduce the strength of NOC so that the speed was significantly reduced at the deep layer. The center of eddy was positioned at 110°E and 6°N, where the cyclonic eddy declined at the deep layer, resulting in the weak VCJ and NOC. These results indicate that the NOC variability took place vertically from the surface layer to the deep layer. According to Huang (1994), based on the distribution of temperature and salinity below 50 m depth, NOC as an off-shelf warm water tongue with lower salinity propagated northward from 4° to 8°N near 112°E. However, the weak NOC profile at the deep layer was influenced by the thermocline existence, which may reduce the effect of wind stress on the water column.

During the first transitional season, the weak ocean currents were dominated in the surrounding the South China Sea and North Natuna Sea. VCJ totally diminished and therefore, the cyclonic eddy could not be generated. During the SEM, the current

profile tended to move northward. This northward current was influenced by the southwesterly wind occurred during the SEM as shown by Maisyarah *et al*. (2019). During the second transitional season, the cyclonic eddy commenced generated from the surface to the deep layer. The generation of cyclonic eddy triggers NOC that will occur during the NWM period.

The structure of eddy in the North Natuna Sea is simpler than the eddy in the South China Sea. In the North Natuna Sea, the cyclonic eddy occur from the surface layer to the deep/bottom layer. As reported by Zhu *et al*. (2019), an eddy with sandwiched circulation occurs in the South China Sea connected to Luzon Strait i.e., anticyclonic in the intermediate layer and cyclonic in the upper and deeper layers, However, the spatio-temporal pattern and the driving mechanisms of the the sandwich circulation remain unclear. These become interesting topics for future studies.

The effect of ENSO on NOC

Figure 5 shows the comparison of the vertical NOC variability during the NWM in the North Natuna Sea. The comparison applied the current vector distribution in January 2011 as a case study of the La Niña event and January 2016 for the El Niño event. Overall, during La Niña, the NOC, the cyclonic eddy, and VCJ were more robust than during the El Niño for all layers and vice versa during El Nino event. Compared to the normal ENSO event shown in Figure 4a-c, NOC during La Niña is stronger than during the normal state while during El Nino is weaker than during the normal state.

The comparison between ocean-atmosphere interactions and the frequency of NOC occurrence is shown in Figure 6. Over the observation period (2006-2016), the NOC's occurrence was identified by the northward current off the Natuna Islands. During La Niña events, the NOC occurred more frequently than during El Niño. During the NWM with strong La Niña in 2007 and 2010, the emergence of NOC was eight times and 11 times, respectively. In contrast, the NOC emerged only four times during El Niño stronger phases. Thus, ocean-atmosphere interactions are influencing the formed NOC magnitude and the frequency of NOC emergence as well.

Since NOC occurrence in the North Natuna Sea is affected by the northerly wind during the NWM as mentioned by Fang *et al*. (2002), the mechanism

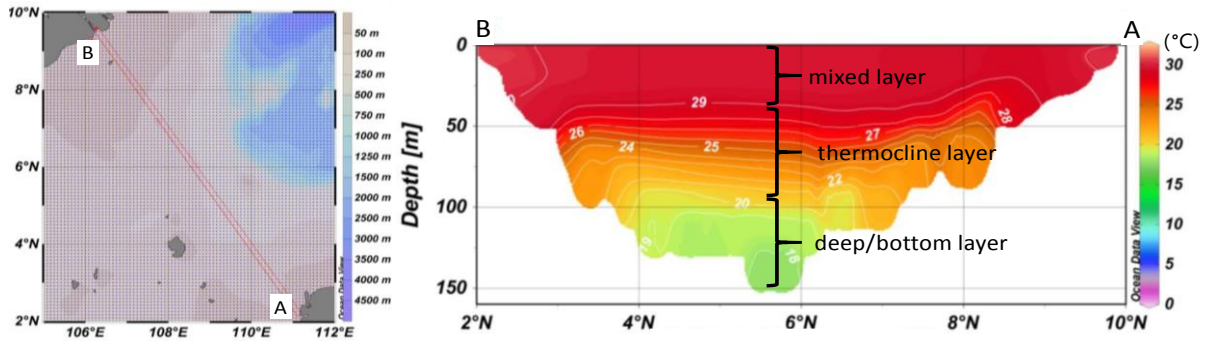

Figure 2. Vertical section of temperature in the North Natuna Sea.

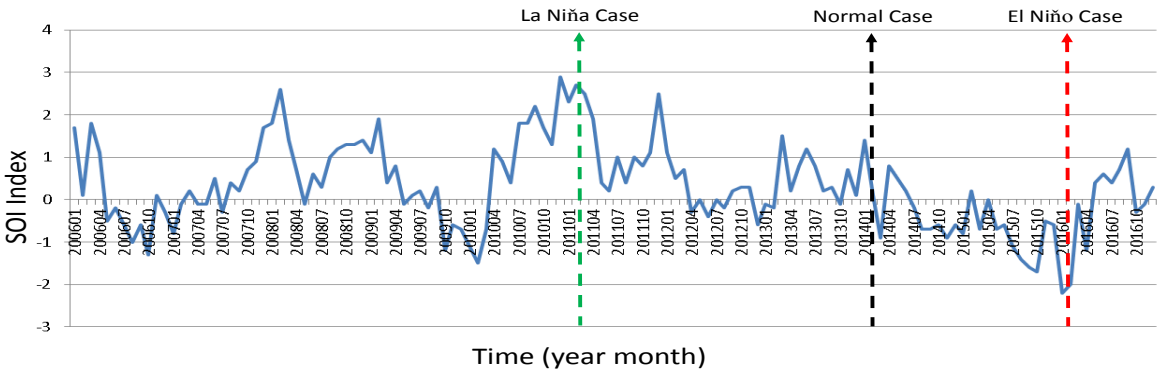

Figure 3. SOI index from 2006 to 2016. Green, black, and red arrows represent the chosen observed period of La Niña, normal condition, and El Niño.

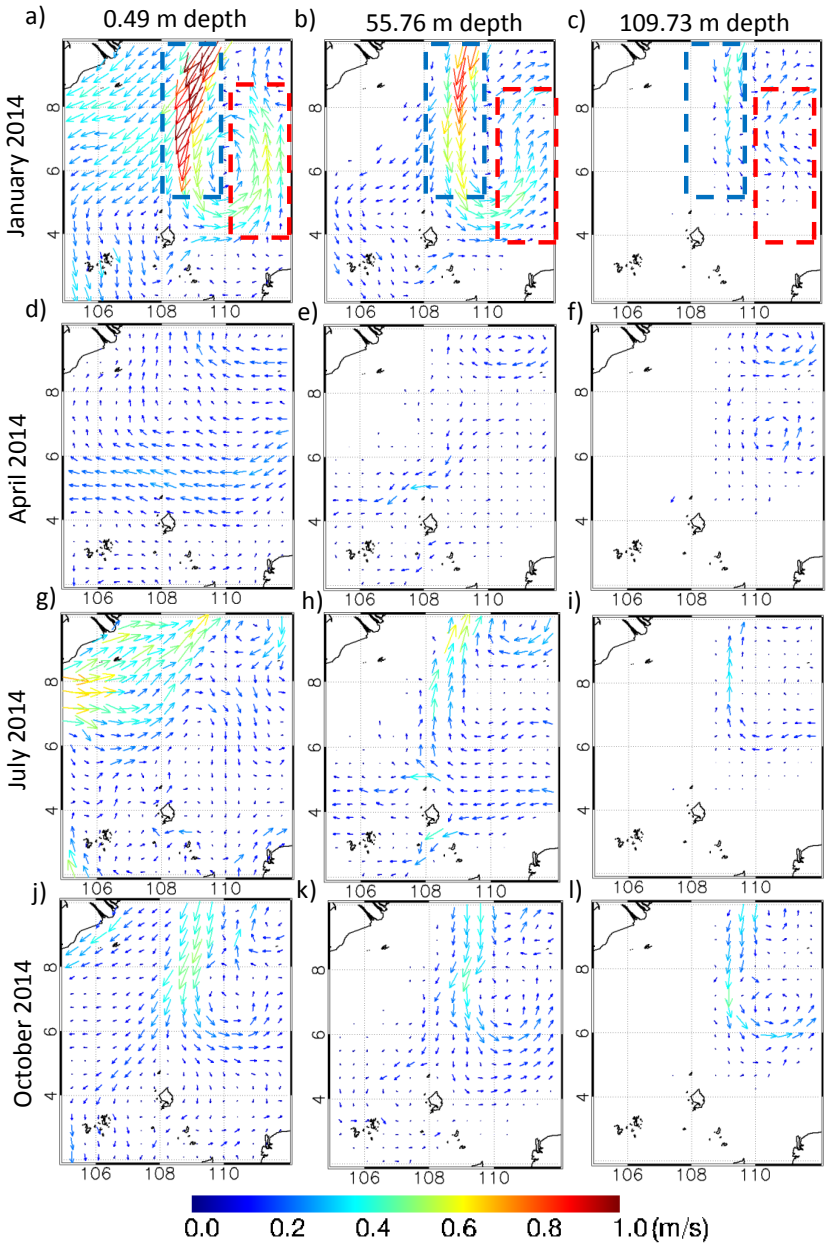

Figure 4. Ocean current pattern in the North Natuna Sea at (a, d, g, j) surface layer, (b, e, h, k) thermocline layer and (c, f, I, l) deep layer during (a, b, c) the NWM, (d, e, f) the first transitional season, (g, h, i) the SEM and (j, k, l) the second transitional season. Dashed red boxes denote NOC and dashed blue boxes denote VCJ.

of ocean-atmosphere interactions-influenced NOC is also related to the wind speed. Figure 7 shows that the northeasterly wind during the NWM was amplified during La Nina with the maximum wind speed reaching 10 $m.s^{-1}$. In contrast, the northeasterly wind was weakened during El Nino with the maximum wind speed was about 8 m/s. The amplified northeasterly wind during the La Nina event piles up much water off the Natuna Islands, accelerating NOC. The weak northeasterly wind during NWM El Nino reduced the convergence of water mass off the Natuna Islands resulting in weakened NOC magnitude. This result is in accordance with Maisyarah *et al*. (2019) which also found the amplified surface wind during La Nina and weakened surface wind during El Nino events that changed SST in this area. Furthermore Zu *et al*. (2019) suggested that not only local wind forcings, but also remote wind stress are important for the interannual variation in the southern South China Sea. Together with Kuroshio intrusion, remote wind forcings influence the circulation and water mass properties in the southern South China Sea through western boundary current advection or VCJ.

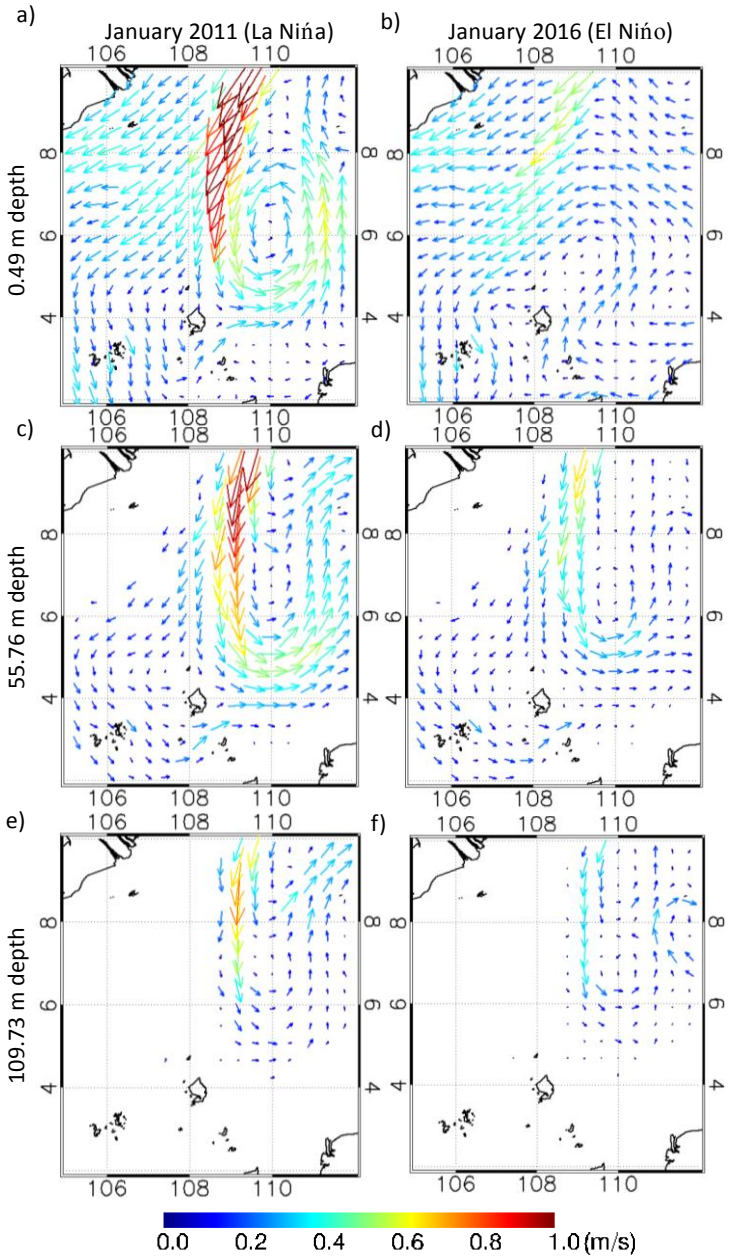

Figure 5. Current pattern distribution at surface layer (a, b), thermocline layer (c, d) and deep layer (e, f) during La Niña (a, c, e) and, El Niño (b, d, f).

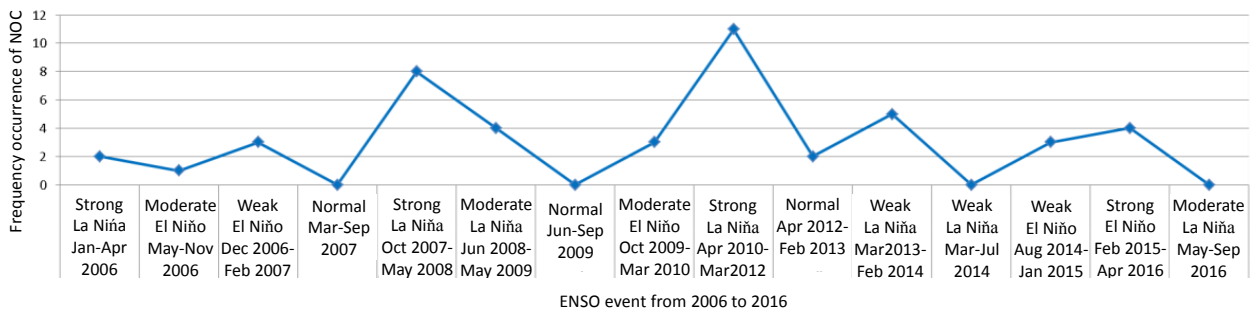

Figure 6. The NOC emergences from 2006 to 2016 in relation with ocean-atmosphere interactions

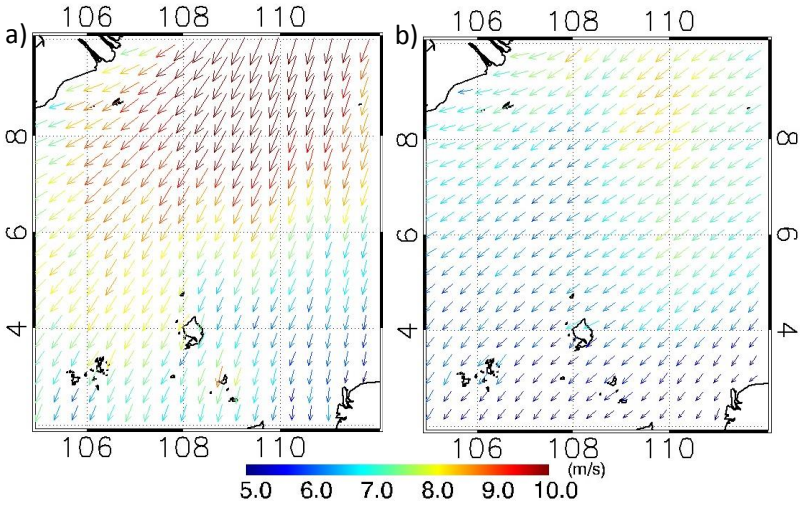

Figure 7. Surface wind pattern distribution during (a) January 2011 (La Niña) and, (b) January 2016 (El Niño)

Conclusion

The variability of NOC in the North Natuna Sea has been studied by using reanalysis data. NOC was commenced to emerge during the second transitional season and reached its peak variability in the NWM season. During the peak of NWM season, NOC can be identified from the surface to the deep/bottom layer with the speed reduction at the deep layer. La Niña tended to amplify NOC through the strengthening of the northeasterly wind speed and vice versa for El Niño. The frequency occurrence of NOC also increased during La Niña and decreased during El Niño.

References

Alifdini, I., Shimada, T. & Wirasatriya, A. 2021. Seasonal Distribution and Variability of Surface Winds in the Indonesian Seas Using Scatterometer and Reanalysis Data. *Int. J. Climatol.,* in press. doi: 10.1002/joc.7101

Chu, P.C., Edmons, N.L. & Fan, C. 1999. Dynamical Mechanisms for the South China Sea Seasonal Circulation and Thermohaline Variabilities. *J. Phys. Oceanogr.,* 29(11):2971-2989

Drévillon, M., Régnier, C., Lellouche, J.M., Garric, G., Bricaud, C. & Hernandez, O. 2018. Quality Information Document For Global Ocean Reanalysis Products GLOBAL-REANALYSIS-PHY-001-030. Marine Copernicus eu.

Fang, W., Fang, G., Shi, P., Huang, Q. & Xie, Q. 2002. Seasonal Structures of Upper Layer Circulation in the Southern South China Sea From in situ Observations. *J. Geophys. Res.,* 107(C11): 23-32. doi: 10.1029/2002JC001343,2002.

Guohong, F., Susanto, D., Soesilo, I., Zheng, Q.A., Fangli, Q. & Zexun, W., 2005. A note on the South China Sea shallow interocean circulation. *Adv. Atmos. Sci.*, 22(6): 946-954.

Fang, G., Wang, Y., Wei, Z., Fang, Y., Qiao, F. & Hu, X., 2009. Interocean Circulation and Heat and Freshwater Budgets of the South China Sea Based on a Numerical Model. *Dyn. Atmosheres Oceans.* 47:55–72

Fernandez, E., & Lellouche, J.M.. 2018. Product User Manual for the Global Ocean Reanalysis Products GLOBAL-REANALYSIS-PHY-001-030. Marine Copernicus eu.

Figa-Saldaña, J., Wilson, J.J., Attema, E., Gelsthorpe, R., Drinkwater, M.R. & Stoffelen, A., 2002. The Advanced Scatterometer (ASCAT) on the Meteorological Operational (MetOp) Platform: A Follow on for European Wind Scatterometers. *Can. J. Remote Sens.,* 28(3): 404-412.

Gan, J., Li, H., Curchitser, E.N., & Haidvogel, D.B. 2006. Modeling South China Sea Circulation: Response to Seasonal Forcing Regimes. *J. Geophys. Res.,* 111: C06034. doi: 10.1029/2005JC003298.

Hu, J., H. Kawamura, H. Hong, & Y. Qi. 2000. A Review on The Currents in the South China Sea: Seasonal Circulation, South China Sea Warm Current and Kuroshio Intrusion. *J. Oceanog.* 56: 607-624.

Huang, Q., 1994. Currents in the Nansha Islands Sea Area, in Proceedings of Physical Oceanography Studies in the Nansha Islands Sea Area, pp. 10–27, China Ocean Press, Beijing.

Khaldun, M.H.I., A. Wirasatriya, A.A.D. Suryo, & Kunarso. 2018. The Influence of Indian Ocean Dipole (IOD) on The Variability of Sea Surface Temperature and Precipitation in Sumatera Island. *IOP Conf. Ser.: Earth Environ. Sci.,* 165(2018): 012008. doi: 10.1088/1755-1315/165/1/012008

Li, L., Xu, J., Jing, C., Wu, R. & Guo, X. 2003. Annual Variation of Sea Surface Height, Dynamic Topography and Circulation in the South China Sea. *Sci. China (series D)*. 46(2):127-138.

Maisyarah, S., Wirasatriya, A., Marwoto, J., Subardjo, P. & Prasetyawan, I.B.. 2019. The Effect of the ENSO on the Variability of SST and Chlorophyll-a in the South China Sea. *IOP Conf. Ser.: Earth Environ. Sci.,* 246: 012027. doi: 10.1088/ 1755-1315/246/1/012027.

Ropelewski, C.F. & Jones, P.D. 1987. An extension of the Tahiti-Darwin Southern Oscillation Index. Monthly Weather Review. 115: 2161-2165.

Setiawan, R.Y. & Habibi, A. 2010. SST Cooling in the Indonesian Seas. *Ilmu Kelautan: Indonesian Journal of Marine Science*. 15(1): 42-46.

Susanto, R.D., Moore, T.S. & Marra, J. 2006. Ocean Color Variability in the Indonesian Seas During the Seawifs era. *Geochem. Geophys. Geosys.,* 7(5):1-16.

Tangang, F.T., Xia, C. & Qiao, F., 2011. Seasonal Circulations in the Malay Peninsula Eastern Continental Shelf from a Wave-tide-circulation Coupled Model. *Ocean Dyn.,* 61: 1317–1328.

Wang, C., Wang, W., Wang, D. & Wang, Q., 2006a. Interannual Variability of the South China Sea Associated with El Niño. *J. Geophys. Res.,* 111: C03023.

Wang, D., Liu, Q., Huang, R., Yan, D., & Qu, T., 2006b. Interannual Variability of the South China Sea Throughflow Inferred from Wind Data and an Ocean Data Assimilation Product. *Geophys. Res. Lett.,* 33: L14605.

Wei, Z., Fang, G., Xu, T., Wang, Y. & Lian, Z. 2016. Seasonal Variability of the Isopycnal Surface Circulation in the South China Sea Derived From a Variable-grid Global Ocean Circulation Model. *Acta Oceanologica Sinica* 35(1): 11–20. doi : 10.1007/s13131-016-0791-3.

Wyrtki, K., 1961. Physical Oceanography of the Southeast Asian Waters, vol. 2, Scientific results of marine investigation of the South China Sea and Gulf of Thailand, NAGA Rep., 195 pp., Scripps Inst. of Oceanogr., La Jolla, Calif.

Xue, H., Chai, F., Pettigrew, N., Xu, D., Shi, M. & Xu, J., 2004. Kuroshio Intrusion and the Circulation in the South China Sea. *J. Geophys. Res.,* 109(C02017):1-14. doi: 10.1029/2002JC001724

Yin, J., C. Liu, J. Zhang, X. Yang, J. Wu, W. Oschmann, F. T. Fürsich, B. Zhu, & H. Zhang. 2018. Distribution and Constraining Factors of Planktonic and Benthic Foraminifers in Bottom Sediments of the Southern South China Sea. *Paleogr. Paleoclimatol. Paleoecol.,* 502:130-146. doi: 10.1016/j.palaeo.2018.04.029.

Zhu, Y., Sun, J., Wang, Y., Li, S., Xu, T., Wei, Z. & Qu, T., 2019. Overview of the Multi-layer Circulation in the South China Sea. *Prog. Oceanogr.*, 175: 171-182. doi: 10.1016/j.pocean.2019. 04.001

Zu, T., Xue, H., Wang, D., Geng, B., Zeng, L., Liu, Q., Chen, J. & He, Y., 2019. Interannual Variation of the South China Sea Circulation During Winter: Intensified in the Southern Basin. *Clim.Dyn.,* doi: 10.1007/s00382-018-4230-3